Open Access Journal

Journal of Power Technologies 97 (3) (2017) 246–251

journal homepage:papers.itc.pw.edu.pl

Performance of the PEM fuel cell module. Part 2. Effect of excess ratio and stack temperature

Janusz T. Cieśliński*, Tomasz Kaczmarczyk, Bartosz Dawidowicz

Gdańsk University of Technology, Narutowicza 11/12, 80233 Gdańsk, Poland

Abstract

The paper describes a fuel cell based system performance under different thermal conditions. The system could be fed with bottled hydrogen or with very high purity hydrogen obtained from reforming of methanol. The system is based on two fuel cell units (1.2 kW each, produced by Ballard Power Systems Inc. and called Nexa), DC/DC converter, DC/AC inverter, microprocessor control unit, load unit, bottled hydrogen supply system and a set of measurement instruments. In this study steady-state operation of the PEM fuel cell system at different values of air excess ratio and different stack temperature was investigated. The load of the system was provided with the aid of a set of resistors. The results obtained show that the net power of the system does not depend on the air excess ratio within the range of λ_{O_2} from 1.9 to 5.0. The polarization curves of the fuel cell module showed that the fuel cell performance was improved with increased stack temperature within the range of 30°C to 65°C. It was established that the total efficiency of the tested system depends on the hydrogen source and is higher when using bottled hydrogen of about 30% and 16%, for minimum and maximum load, respectively.

Keywords: PEMFC, Hydrogen, Methanol reforming, Operating temperature, Excess ratio

1. Introduction

The priority goal for energy conversion engineers is to develop highly efficient, low emission energy systems. One promising technology involves fuel cells which convert chemical energy directly into electrical energy. Energy conversion using fuel cells is very efficient, with only a small negative impact on the environment. Fuel cells can be used either in power plants or in dispersed generation [1].

The Polymer Electrolyte Fuel Cell (PEFC) also known as the Proton Exchange Membrane and the Polymer Electrolyte Membrane (PEM) fuel cells have been used for many years in small scale mobile solutions as energy sources for laptop computers, small transport devices such as forklifts and military equipment. Since the continued development of fuel cells is leading to to lower prices and higher efficiencies, this technology can also be used in large stationary applications. PEM fuel cells are viewed as one of the most environmentally friendly propulsion systems for automotive travel in the future [2, 3].

Cell performance for any fuel cell is a function of pressure, temperature, reactant gas composition and utilization [1]. In order to ensure long-life operation and durability of PEM fuel cells [4] the ratio between the oxygen consumed in the electrochemical reaction and the oxygen flow rate supplied to the fuel cell must fulfil the stoichiometric relation required to produce the current demanded, otherwise a phenomenon called oxygen starvation occurs [5]. When starved of fuel or oxygen, fuel cell performance degrades and cell voltage drops. Oxygen starvation occurs when oxygen partial pressure falls below a critical level in any location at the cathode [6]. This results in a rapid cell voltage decrease and can cause a burn through the surface of the membrane. Therefore regulation of the oxygen excess ratio - defined as the ratio of the oxygen entering the cathode and the oxygen reacting in the fuel cell stack [6] - is a crucial issue [7, 8]. The desired value of the oxygen excess ratio depends on the fuel cell itself and on the operating objective. To guarantee safety and high efficiency of the stack, the literature value of $\lambda_{O_2} = 2$ is proposed [9]. Notice that positive deviations of λ_{O_2} above the reference imply lower efficiency [1, 8]. Zhang et al. [10], in turn, presented the effects of temperature and the equivalent internal resistance on the output characteristics of PEM fuel cells. The proposed semi-empirical dynamic model is constructed based on measurements from a Nexa^{TM} PEM fuel cell power module under different load conditions, and the model has been validated by static as well as dynamic

*Corresponding author
Email address: jcieslin@pg.gda.pl (Janusz T. Cieśliński)

tests. The effects of temperature and variations in the internal impedance under different load conditions have been studied. The results indicated that the model provides an accurate representation of the dynamic and static behaviors of the fuel cell power module. Xue et al. [11] considered the effect of temperature transient behavior in their modeling of PEM fuel cell performance. Their model incorporates the complicated temperature, gas flow and capacitance effects under operating conditions. The focus was on the dynamic and transient properties of the system. They used the control volume approach to develop a set of equations that govern the system dynamics. The fuel cell system was divided into three control volumes: the anode channel, the cathode channel, and the fuel cell body. For each control volume, the establishment of a lumped-parameter dynamic model was realized using a combination of intrinsic mechanistic relations and empirical modelling. Recently, Beicha and Zaamouche [12] developed a model to predict the efficiency and power of the fuel cell as a function of operational parameters of the cell, like temperature, partial pressures and membrane humidity.

PEM fuel cells work on pure hydrogen as a fuel (at least 99.99% purity) and most often ambient air is used as the oxidizer. It is a fact that methods to produce hydrogen for fuel cells are being developed. The hydrogen can be produced by electrolysis, direct reforming of methane, thermal decomposition of water or biomass.

To produce high purity hydrogen from energy carriers such as alcohol, reformers are designed. Methanol, an alcohol, can be used to produce hydrogen. It is easier and safer to store methanol than hydrogen, therefore it makes fuel cell systems more useful for potential users.

Methanol is a preferred fuel for fuel cells [13–15], as it features high energy density, low manufacturing cost, and straightforward storage and distribution [16].

There are two approaches to using methanol in fuel cells. Firstly, fuel cell could be supplied with methanol directly [17–21] or, secondly after converting methanol into hydrogen-rich gas through the reforming process [22, 23].

The objective of this study was to provide steady-state characteristics of the Nexa module for different values of the air excess ratio, operating temperature and hydrogen source.

2. Experimental setup

2.1. Fuel cell module and apparatus

The Nexa power module produces unregulated DC power for interfacing with external power conditioning equipment. A single fuel cell element produces about 1 volt in open-circuit and about 0.6 volts at full current output. The Nexa fuel cell stack has a total of 47 fuel cells in series. The geometric area of the single cell is 120 cm^2. The unit is equipped with an air compressor and cooling blower. The main specifications of the fuel cell module are summarized in Tab. 1.

The system consists of the two fuel cell units (1.2 kW each), methanol reformer, DC/DC converter, DC/AC inverter

Table 1: Technical specifications of the Nexa fuel cell module [24]

Performance	Rated net output, W	1,200
	Heat dissipation, W	1,600
	Current, A DC	46
	Voltage, V DC	26
	Lifetime, h	1,500
Fuel	Gaseous hydrogen, % dry	99.99
	Supply pressure, MPa	0.7 to 1.72
Operating environment	Ambient temp., ° C	3 to 40
	Humidity, % non -condensing	0 to 95
Emissions	Pure water (vapor and liquid), ml/h	Maximum 870
	CO, CO2, NOx, SO2 particulate, ppm	0

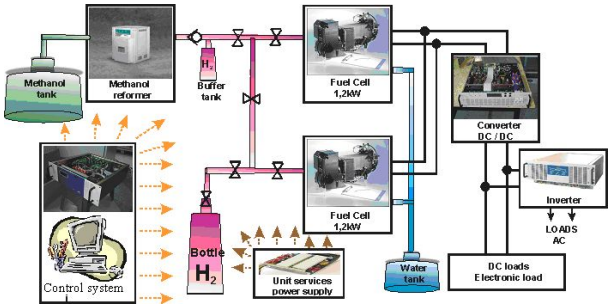

Figure 1: Schematic of the fuel cell module

and microprocessor control unit—Fig. 1. The system investigated is designed as a duel fuel. It is possible to feed the fuel cell directly with hydrogen from a gas cylinder or with hydrogen from methanol reforming. General requirements for this test bench related to performing all electrical and non-electrical measurement connected with electricity production.

The system is equipped with flow meters (for methanol, hydrogen and air), temperature and humidity sensors, oxygen concentration counters and all voltages and currents measurement devices (Fig. 1). The control unit based on a DSP microprocessor acts as a central data acquisition unit and controls the operation of the whole system. View of the tested PEM fuel cell system is shown in Fig. 2.

2.2. Methanol reforming

Hydrocarbons reforming is the most commonly used method to obtain pure, cheap hydrogen on a large industrial scale. The fundamental principle underlying this process is the highly endothermic reaction between steam and hydrocarbons occurring at temperatures of over 700°C. Temperatures that high lead to many technological problems. The use of catalysts lowers the temperature of the reaction to below 400°C. The most common catalysts are compounds of nickel Ni with copper Cu or zinc Zn and chromium Cr [22, 25]. Overall, the chemical reaction of steam reforming of hydrocarbons can be written as:

$$C_nH_n + nH_2O \rightarrow nCO + (\frac{m}{2} + n)H_2 \quad (1)$$

The products of this reaction are carbon monoxide and hydrogen. In the next step CO goes into reaction with water

Figure 2: View of the module

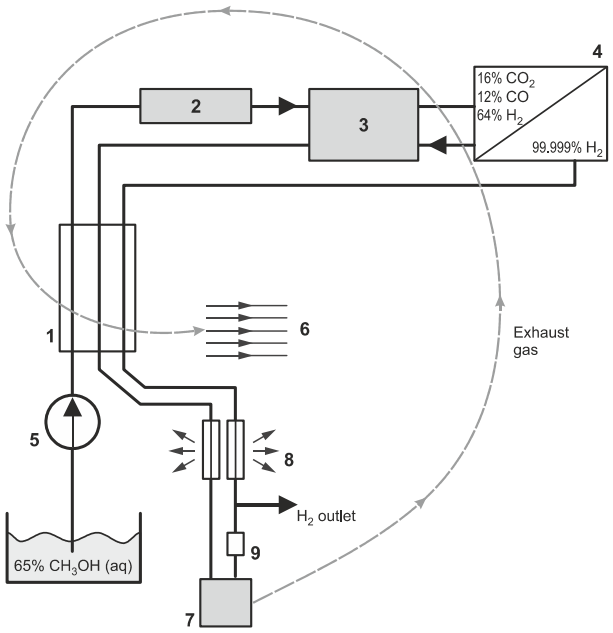

Figure 3: Schematic of the Genesis Fueltech 20L reformer;1—preheater, 2 - boiler, 3—catalyst bed, 4—separating membrane, 5—pump, 6—flue gas, 7—catalytic burner, 8—cooler, 9 - valve

H_2O producing carbon dioxide CO_2 and hydrogen. This is called a shift reaction:

$$CO + H_2O \rightarrow CO_2 + H_2 \tag{2}$$

For methanol CH_3OH chemical reactions can be written as:

$$\begin{aligned} CH_3OH &\rightarrow CO + 2H_2 \\ CO + H_2O &\rightarrow CO_2 + H_2 \end{aligned} \tag{3}$$

and globally

$$CH_3OH + H_2O \rightarrow CO_2 + 3H_2 \tag{4}$$

In real devices the molar ratio of water H_2O to carbon C is about 2.5:1 and results from the imperfection of the reaction and the need to restrict soot generation.

2.3. Genesis Fueltech 20L methanol reformer

The tested system is equipped with a Genesis Fueltech 20L reformer—Fig. 3. This device was installed in a non-military application for the first time and has the serial No. of 0005. As mentioned above, in order to perform the reforming reaction at low temperature there is a need to use highly active catalysts. The most important feature of this substance in this application is high chemical activity and resistance to chemical deterioration in the presence of sulfur. To use steam reforming technology in such a small device, Genesis Fueltech developed their own catalyst in the form of small balls with a porous surface. The chemical composition of the catalyst is not known, but most of the catalysts on the market are based on nickel Ni.

The reforming process in the 20L reformer—Fig. 3 starts with the intake of a small amount of 65% water solution of methanol by a pump (5). The liquid solution is heated up in the pre-heater (1) and evaporates in a boiler (2). The next step is the reforming reaction that takes place in the catalyst bed (3). The products of the reaction are 64% H_2, 12% CO, 16% CO_2 and steam.
The composition of the raffinate leaving the catalyst bed (3) makes it unsuited for use as a fuel in a low temperature fuel cell due to its very high (12%) content of carbon monoxide CO. There are many solutions to this problem, but the Genesis Fueltech reformer uses a separation membrane made with palladium and silver (4), which allows only hydrogen H_2 molecules to pass freely. On the other side of the membrane the hydrogen has purity of over 99.999% which is sufficient to feed it into the PEM. The hydrogen is routed to the cooler (8) and then can be used in the fuel cell.

The rest of the raffinate that did not pass through the membrane returns to the catalyst bed (3) and then proceeds to the preheater (1), heating up the methanol solution. The next step is catalytic combustion in a burner (7), where the rest of the raffinate is burned to drive the whole reforming process. The flue gas goes around the heating surfaces in the reformer and escapes through a valve located on the reverse side of the reformer.

3. Results

The steady state polarization curve shown in Fig. 4 shows regions where there are stable steady states that could exist for the same set of operating parameters (feed flow rate,

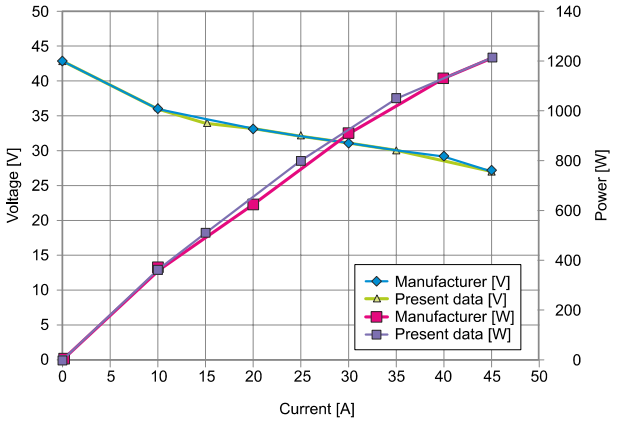

Figure 4: Steady-state characteristics

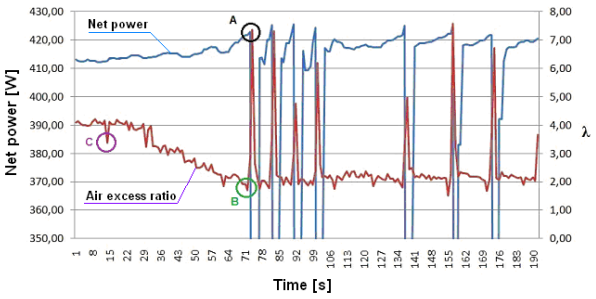

Figure 5: Power of the fuel cell and air excess ratio versus time

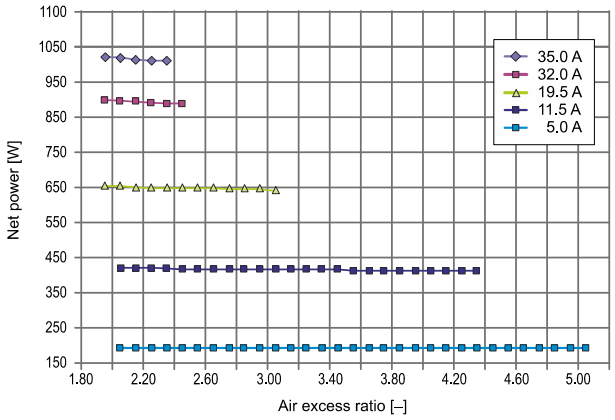

Figure 6: Power of the fuel cell versus air excess ratio

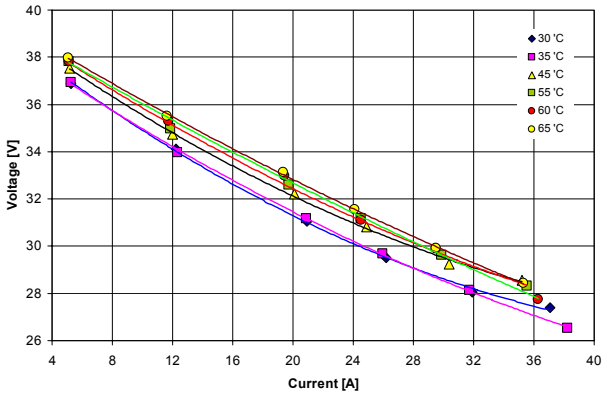

Figure 7: Effect of the operation temperature on the polarization curves

temperature and load resistance). The results are in good agreement with manufacturers data [24].

As an example Fig. 5 shows the power of the fuel cell and simultaneously the air excess ratio against time for the lowest resistive load tested. For each set of resistors (load) three characteristic points can be distinguished; every about 15 seconds—point C, a drop in air excess ratio value has been observed, independent of load and air volume flow rate. For air excess ratio value below 1.9 the power of the fuel cell increased considerably, nevertheless the on-board control system and software for measuring and collecting data of internal states (delivered by the manufacturer) switched the system off—point A in Fig. 5, and after a very short time switched the system back on and as a result the air excess ratio reached a very high value—point B in Fig. 5.

Fig. 6 shows the power of the Nexa fuel cell as a function of air excess ratio for 5 loads (current values), i.e. 35 A, 32 A, 19.5 A, 11.5 A and 5 A. Contrary to [26], power of the tested Nexa fuel cell slightly decreases with the increase in air excess ratio, about 1-1.5% with λ_{O_2} increase from 1.9 to 5.2. According to [8] a dramatic drop in net power of the Nexa module depends on stack current and there exists an optimal value of λ_{O_2} by which maximum net power is obtained. For instance, for stack current 30 A and 5 A, the optimum air excess ratio is about 2 and 5, respectively.

Fig. 7 illustrates the polarization curves of a fuel cell at several operating temperatures with the range of 30°C to 65°C. These curves indicate that fuel cell performance improved as operating temperature increased. The improvement in fuel cell stack performance with increasing operating temperature, in terms of the measured voltage, can be explained by the increase in gas diffusivity and membrane conductivity at higher temperatures. Since gas diffusivity improves with increasing fuel cell temperature, fuel cell stack performance is improved at higher temperatures. As a result the reaction kinetics are improved [27].

Fig. 8 shows voltage and current output as a function of stack power. The operating temperature of the fuel cell was changed from 30°C to 65°C. Current output increases almost linearly with stack power, reading about 38 A for power output 1015 W. Simultaneously, the recorded voltage drops from 38 V to 27 V for minimum and maximum power output, respectively.

Fig. 9 shows the effect of operating temperature on the power of the fuel cell. Electrical power decreases slightly with an increase in stack temperature from 1015 W for 30°C to 1004 W for 65°C.

Fig. 10 shows the efficiency of the reformer as the ratio of

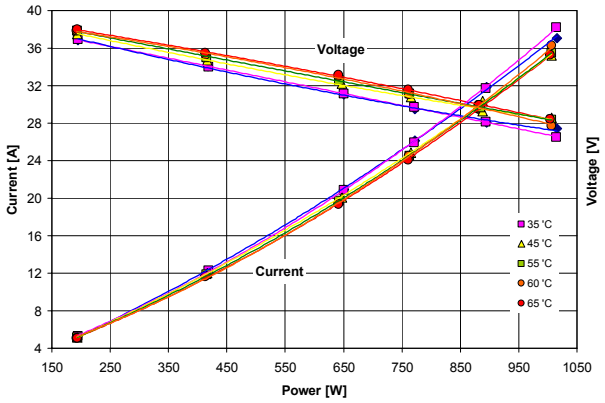

Figure 8: Effect of operating temperature on the performance of the fuel cell

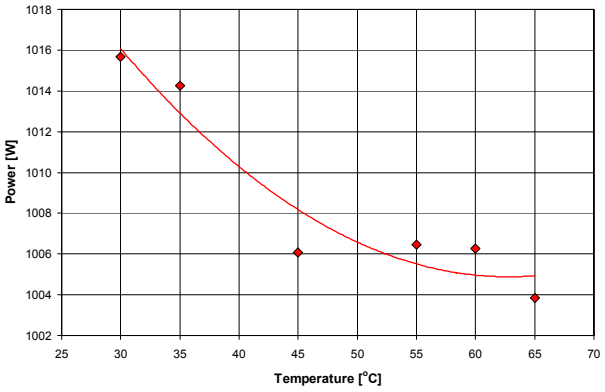

Figure 9: Effect of operating stack temperature on the power of the fuel cell

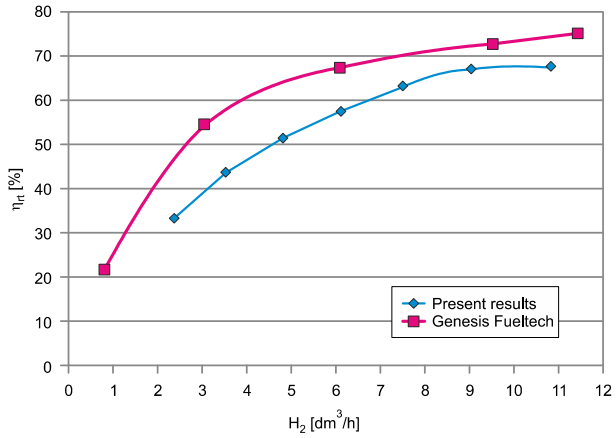

Figure 10: Efficiency of the methanol reformer

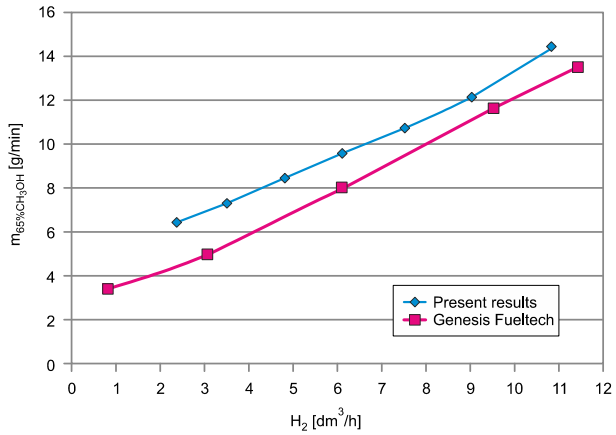

Figure 11: Mixture of ethanol/water consumption versus volume flow rate of hydrogen generated

chemical energy of hydrogen generated to chemical energy of the 65% water solution of methanol supplied to the reformer. The results are lower than the manufacturer's data. Reformer efficiency depends on module load (hydrogen consumption)—the higher the load applied, the higher the efficiency observed. This is because the reformer needs an almost constant amount of energy to keep the process going [28, 29]. Minimum and maximum efficiency of the reformer is 35% and about 80% for minimum (2 dm^3/min) and maximum (11 dm^3/min) hydrogen generation, respectively.

As an example Fig. 11 shows consumption of the ethanol/water mixture against the hydrogen volume flow rate generated. The results obtained in this study show that the actual consumption of the ethanol/water mixture is higher than that presented in the producer's characteristics, probably because of the decrease in reformer catalyst bed activity.

Fig. 12 illustrates the total efficiency of the module examined while working on hydrogen from the gas bottle and hydrogen produced by the reformer. Total efficiency is defined as the ratio of electrical power output to chemical energy of the methanol solution or hydrogen. The efficiency of the module while working on the methanol produced hydrogen is only 15% for minimum hydrogen volume flow rate 2.3 dm^3/min. When using gas bottle hydrogen efficiency increases to 45%. The higher the reformer output (hydrogen volume flow rate) the smaller the efficiency difference. For the maximum tested load of the module, i.e. 10.8 dm^3/min of corresponding hydrogen consumption, the total efficiency of the module was 30% and 46% for hydrogen from methanol reforming and the gas cylinder, respectively.

4. Conclusions

The efficiency of the fuel cells obtained during our tests is similar to data from the manufacturer, Ballard.

The fuel cell module tested has quite a high internal load. For nominal power of 1.2 kW almost 300 W has to be used to keep the system working, which dramatically reduces overall efficiency.

The results obtained show that the power of the Nexa fuel cell decreases slightly—by about 1–1.5%—as the air excess ratio increases from 1.9 to 5.2.

The polarization curves of the fuel cell show that fuel cell performance improved as stack temperature increased. The power of the fuel cell module decreases as stack temperature increases.

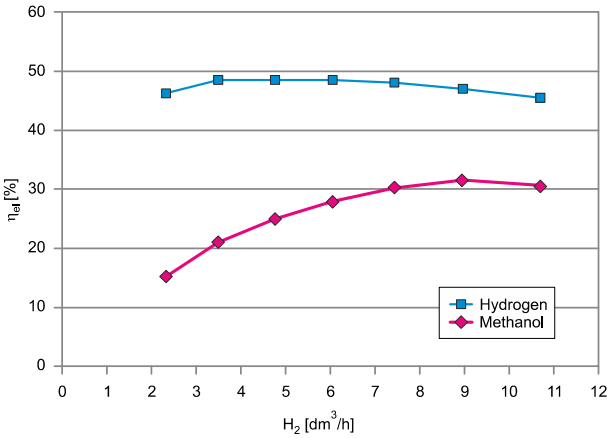

Figure 12: Total efficiency of the module versus volume flow rate of hydrogen generated

The efficiency of the methanol reformer depends on its capacity and changed from 33% to 78% for minimum and maximum load, respectively.

The purity of the hydrogen produced by the tested reformer is satisfactory across the whole capacity range.

Nexa modules are thermally protected. For nominal power output (1.2 kW) the working temperature is below 70°C. Improvement of the cooling system could lead to higher power, probably about 1.5 kW and current of 75A.

References

[1] K. Kordesh, S. G, Fuel cells and their applications, VCH, Weinheim, 1996.

[2] P. Corbo, F. Migliardini, O. Veneri, An experimental study of a pem fuel cell power train for urban bus application, Journal of Power Sources 181 (2) (2008) 363–370.

[3] P. Pei, Q. Chang, T. Tang, A quick evaluating method for automotive fuel cell lifetime, International Journal of Hydrogen Energy 33 (14) (2008) 3829–3836.

[4] W. Schmittinger, A. Vahidi, A review of the main parameters influencing long-term performance and durability of pem fuel cells, Journal of Power Sources 180 (1) (2008) 1–14.

[5] J. Gruber, M. Doll, C. Bordons, Design and experimental validation of a constrained mpc for the air feed of a fuel cell, Control Engineering Practice 17 (8) (2009) 874–885.

[6] J. T. Pukrushpan, A. G. Stefanopoulou, H. Peng, Control of fuel cell breathing, Control Systems, IEEE 24 (2) (2004) 30–46.

[7] W. Garcia-Gabin, F. Dorado, C. Bordons, Real-time implementation of a sliding mode controller for air supply on a pem fuel cell, Journal of process control 20 (3) (2010) 325–336.

[8] M. Wendeker, A. Malek, J. Czarnigowski, R. Taccani, P. Boulet, F. Breaban, Adaptive airflow control of the pem fuel cell system, Tech. rep., SAE Technical Paper (2007).

[9] Q. Chen, L. Gao, R. A. Dougal, S. Quan, Multiple model predictive control for a hybrid proton exchange membrane fuel cell system, Journal of Power Sources 191 (2) (2009) 473–482.

[10] Z. Zhang, X. Huang, J. Jiang, B. Wu, An improved dynamic model considering effects of temperature and equivalent internal resistance for pem fuel cell power modules, Journal of Power Sources 161 (2) (2006) 1062–1068.

[11] X. Xue, J. Tang, A. Smirnova, R. England, N. Sammes, System level lumped-parameter dynamic modeling of pem fuel cell, Journal of Power Sources 133 (2) (2004) 188–204.

[12] A. Beicha, R. Zaamouche, Electrochemical model for proton exchange membrane fuel cells systems, Journal of Power Technologies 93 (1) (2013) 27.

[13] R. O'Hayre, S. Cha, W. Colella, P. F, Fuel cell fundamentals, John Wiley & Sons, Inc, New York, 2009.

[14] J. Milewski, J. Lewandoski, Biofuels as fuels for high temperature fuel cells, Journal of Power Technologies 93 (5) (2013) 347.

[15] J. Milewski, K. Michalska, A. Kacprzak, Dairy biogas as fuel for a molten carbonate fuel cell-initial study, Journal of Power Technologies 93 (3) (2013) 161.

[16] R. Metkemeijer, P. Achard, Comparison of ammonia and methanol applied indirectly in a hydrogen fuel cell, International journal of hydrogen energy 19 (6) (1994) 535–542.

[17] Valdez T.I. and Narayanan S.R.: Recent studies on methanol crossover in liquid-feed direct methanol fuel cells, http://trs-new.jpl.nasa.gov/dspace/bit stream /2014/20662/1/98-1710.pdf.

[18] U. Krewer, Y. Song, K. Sundmacher, V. John, R. Lübke, G. Matthies, L. Tobiska, Direct methanol fuel cell (dmfc): analysis of residence time behaviour of anodic flow bed, Chemical Engineering Science 59 (1) (2004) 119–130.

[19] V. Oliveira, C. Rangel, A. Pinto, Modelling and experimental studies on a direct methanol fuel cell working under low methanol crossover and high methanol concentrations, international journal of hydrogen energy 34 (15) (2009) 6443–6451.

[20] A. Trendewicz, J. Milewski, An innovative method of modeling direct methanol fuel cells, Journal of Power Technologies 92 (1) (2012) 20.

[21] D. Falcão, V. Oliveira, C. Rangel, A. Pinto, Experimental and modeling studies of a micro direct methanol fuel cell, Renewable Energy 74 (2015) 464–470.

[22] K. Geissler, E. Newson, F. Vogel, T. Truong, P. Hottinger, Kinetics and systems analysis for producing hydrogen from methanol and hydrocarbons, Volume V General Energy 5 (1) (2001) 8.

[23] C.-H. Fu, J. C. Wu, Mathematical simulation of hydrogen production via methanol steam reforming using double-jacketed membrane reactor, International Journal of Hydrogen Energy 32 (18) (2007) 4830–4839.

[24] Nexa Power Module User's Manual, Ballard Power Systems, June 2003.

[25] DeVries D.: Data Sets and Modeling Comparisons Model 20L Reformer, Genesis Fueltech 2006.

[26] D. Wecel, PEMFC cooperating with PV and hydrogen generator with the use of waste heat. Systemy, technologie i urządzenia energetyczne., Vol. 1, Kraków, in Polish.

[27] J. Zhang, Y. Tang, C. Song, X. Cheng, J. Zhang, H. Wang, Pem fuel cells operated at 0% relative humidity in the temperature range of 23–120 c, Electrochimica Acta 52 (15) (2007) 5095–5101.

[28] A. F. Ghenciu, Fuel processing catalysts for hydrogen reformate generation for pem fuel cells, Fuel Cell (2004) 17–19.

[29] F. Fernandes, A. Soares Jr, Modeling of methane steam reforming in a palladium membrane reactor, Latin American applied research 36 (3) (2006) 155–161.